

Research article

Low-temperature Magnetic Properties of 100- 110- and 111-crystal Oriented BiFeO₃ Epitaxial Thin Film

Tahta Amrillah^{1,2*}, Jen-Yih Juang²¹Department of Nanotechnology, Faculty of Advanced Technology and Multidiscipline, Universitas Airlangga, Surabaya 60115, Indonesia²Department of Electrophysics, National Chiao Tung University, Hsinchu 30010, Taiwan

Article info

Keywords:

Multiferroic
Spintronics
Epitaxy
Thin-film
Magnetic

Abstract

BiFeO₃ (BFO) is extensively studied multiferroic material that possible to be integrated in next generation spintronics device. In this present research, BFO has been epitaxially grown on SrTiO₃ (STO) substrates having various crystal orientations; (100), (110), and (111). We found that the lattice matching hold a pivotal factor in the epitaxial stabilization of BFO thin film. We also found that the magnetic properties of BFO thin film having various crystal orientations at below room temperature are different due to several reason, such as strain effect and crystal orientations.

1. Introduction

BiFeO₃ (BFO) is well recognized as an excellent room-temperature multiferroic material. BFO is predicted could be utilized as a multiferroic layer integrated into the so-called magnetoelectric random access memory (MERAM) device to control the magnetic spin *via* applied voltage [1]. Nevertheless, BFO has weak magnetic strength, with *G*-type antiferromagnetically spin alignment at room temperature [2]. In the low temperature, the magnetic structure of BFO becomes more complicated exhibiting a spin-glass behavior [3]. Various developments have been devoted to studying and modifying the magnetic properties of BFO [4]. For instance, epitaxial growth of BFO on various substrates, which in turn, not only modify the crystal structures but also strongly influence the magnetic properties of BFO [4–6].

In this present research, BFO is epitaxially grown on various orientations of single crystal SrTiO₃ (STO) substrates to understand the hidden magnetic properties, especially for their low-temperature ferromagnetism which rarely been studied previously. We found that the spin-glass behavior of BFO varies due to several reason, such as strain effect and crystal orientations, etc. The correlation between the crystal orientations, and its implication on the low temperature magnetic properties is discussed by comparing the phase, microstructures, and the magnetic properties of the BFO grown on on the STO (001), -(110), and -(111) substrates.

2. Experimental Methods

The BFO thin films were synthesized *via* epitaxial growth on the STO (001), -(110), and -(111) substrates by the pulsed laser deposition (PLD) technique as schematically shown in Figure 1.

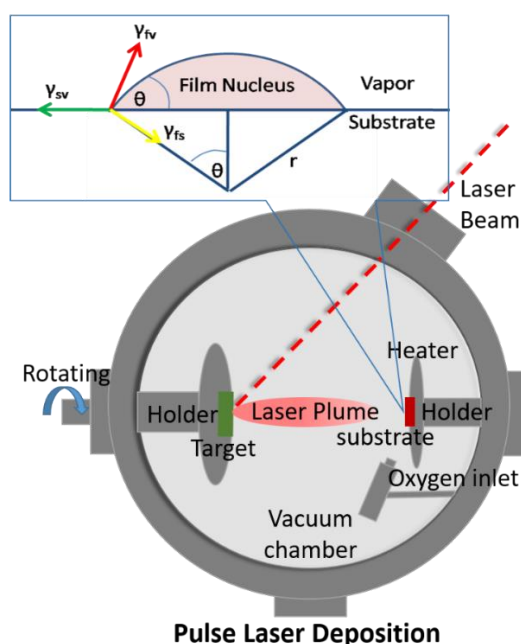


Fig. 1. Schematic set up and experiment of PLD method

*Corresponding author
Email: tahta.amrillah@stmm.unair.ac.id

A single target of BFO was used to grow the films. During the PLD process, a KrF laser (248 nm) with a laser energy density of 0.5 J/cm² and a repetition rate of about 10 Hz was used to ablate the target, whereas the STO substrates were maintained at 600 °C in an oxygen pressure of 100 mTorr. X-ray diffraction (XRD) and atomic force microscopy (AFM) were utilized to understand the details of the phase, structure, and topographic/roughness of the films. Temperature-dependent magnetization is measured with a Quantum Design superconducting quantum-interference device (SQUID) magnetometer, with applied magnetic field about 500 Oe along in-plane direction of the film.

3. Results and Discussion

Figure 2 show XRD results of BFO grown on the STO (100), -(110), and -(111) substrates (black, red, and blue line, respectively). Hereafter, these films are labeled as BFO/STO (100), BFO/STO (110), and BFO/STO (111) samples. BFO and STO substrates interface conditions essentially hold a pivotal role for phase stabilization of the thin film [2, 5, 7]. During the epitaxial growth, the crystalline arrangement and phase formation of BFO thin film are significantly affected by lattice matching [2, 7], because the BFO is isostructural with STO having a small lattice mismatch of around 1.3% with respect to their bulk value. Nevertheless, several factors also need to be considered such as the surface energy and structure continuity rendering a favorable crystalline growth direction, as well as the chemical bonding, drive the in-plane rotation to impose the phase formation of the BFO phase. Thus, since BFO and STO are having a similar crystal structure, therefore, the BFO thin film is crystallized following the crystal orientation of STO substrates.

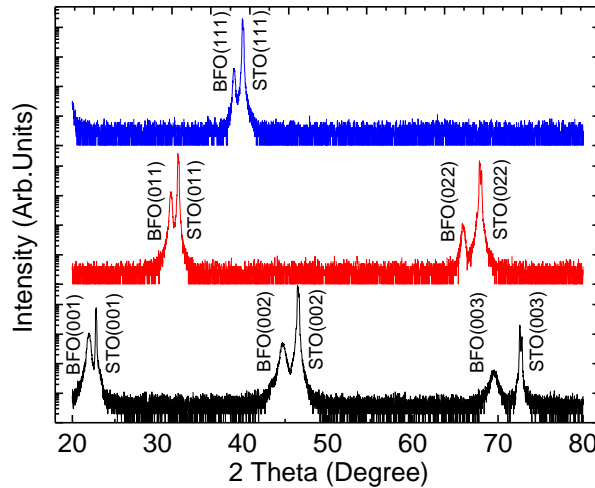


Fig. 2. XRD results of BFO/STO (100), BFO/STO (110), and BFO/STO (111) samples (black, red, and blue lines, respectively)

Figure 3 shows AFM results of the BFO/STO (100), BFO/STO (110), and BFO/STO (111) samples. The surface morphology of the BFO thin film appears to vary with the orientation of the STO substrates. In addition to lattice matching, it is important to note that the epitaxial stabilization is also strongly associated with the surface energy and structural continuity resulted from BFO and the STO substrates. The BFO will adjust their crystal structure to satisfied a small differences in surface energy with the STO substrates. However, when strain energy from lattice mismatch of film and substrate arises, it can lead to a transition of the layer-by-layer growth to island-like growth [2], hence, the surface roughness increases. Though the lattice matching of BFO and STO substrate is small, however, the lattice mismatch among the BFO with those different crystal oriented STO substrates are different [8]. Therefore, different amounts of misfit strain to BFO from STO(001), -(110), and -(111) substrates induce different surface morphologies of BFO thin films, as shown in AFM results. In addition, the polar surface also affects the surface morphology of the thin film [9, 10]. Here, STO(100) has non-polar surface, while -(110), and -(111) have polar surface. It has been reported a distinct island nucleation kinetics in different surface polarities, wherein, the early stage island nucleation contributes to the final surface morphology of the film [10].

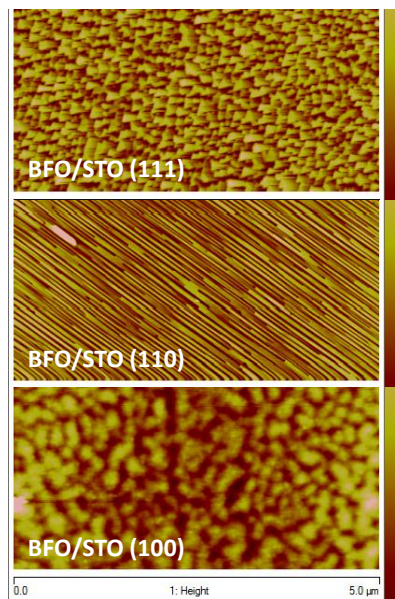


Fig. 3. AFM results of BFO/STO (100), BFO/STO (110), and BFO/STO (111) samples

Figure 4 shows temperature-dependent magnetization (M-T) of the BFO/STO (100), BFO/STO (110), and BFO/STO (111) samples. Similar to that observed in the BFO single crystal, the M-T results of all samples are showing magnetic phase transitions. For BFO single crystal, at least there are four magnetic and dielectric anomalies were obtained at 50 K, 140 K, 200 K, and 230 K [11]. It has been further identified that the anomalies at 50 K is related to the spin glass behaviour and with magnetoelectric coupling, whereas the transition at 140 K, 200 K, and 230 K were dominantly magnetic, magnetoelastic with small coupling to polarization, and spin glass behaviour, respectively. As for BFO thin film samples in this present research, the FC and ZFC curves start to split around 160 K for all samples due to the presence of spin glass behaviour [11]. It was also observed transition at ~42 K for BFO/STO (111) and -(110), while ~46 K for BFO/STO (100). The difference in this magnetic transition may be related to strain effects, wherein, the BFO on STO (100) has more compressive strain compare to BFO on STO (111) and -(110) substrates.

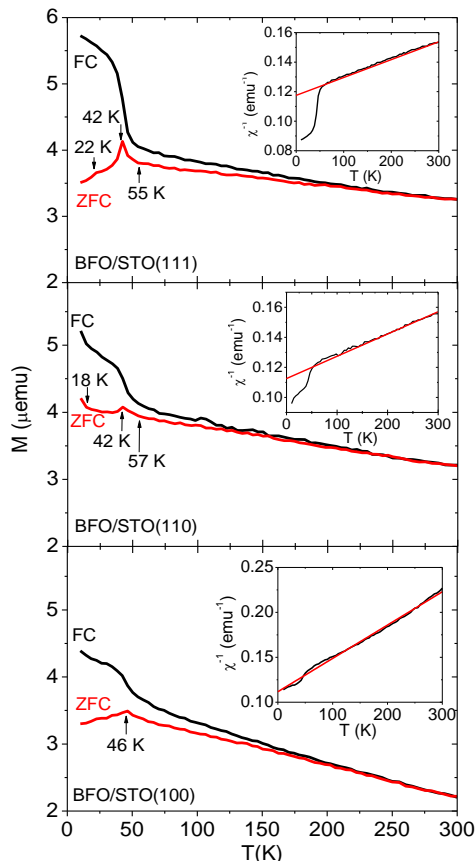


Fig. 4. M-T results of BFO/STO (100) (lower panel), BFO/STO (110) (middle panel), and BFO/STO (111) (upper panel) samples

Furthermore, there are second magnetic transition of BFO/STO (111) and BFO/STO (110) (at 22 K and 18 K, respectively) that probably absence in BFO/STO (100). Again, it may be due to different strain impose crystal structure of BFO thin film, since STO (100) give larger in-plane strain to the BFO thin film compare than STO (111) and -(110) substrates [8]. Complicated magnetic structure of BFO at below room temperature may open up further study which then important to understand another multiferroic system. For instance, large magnetization enhancement of BFO on STO (111) substrate at ~55 K may become interesting feature that possible to pave the way creating BFO with strong magnetic properties. According to the crystal and magnetic structures of BFO, it was well recognized that BFO has a G-type antiferromagnetic, wherein, their spins are ferromagnetically aligned in the (111) plane [11]. Therefore, it also may caused the observed largest magnetic moment in our BFO/STO (111) sample compare to other samples.

The observed FC curve in the M-T results of BFO/STO (100) and -(110) samples are typical [12], while for sample BFO/STO (111), a continuous upward curvature is observed which might be indicate a ferromagnetic-like spin structure. Nevertheless, according to the χ^{-1} -T plot of FC curve obtained from the Curie-Weiss law (inset Figure 4), the estimated Curie temperature, θ , is found to be negative in all the samples which indicate the antiferromagnetic interactions [12]. The negative θ are also related to other peculiar magnetic behaviors such as a short-range ferromagnetism, spin-cluster character spindisorder as well as superparamagnetism [12].

4. Conclusions

BFO thin film with different crystal orientation have successfully synthesized on top of STO substrates with different crystal orientation (100, 110, and 111) using PLD method. We found that the spin-glass behavior of BFO varies due to several reason, such as strain effect and crystal orientations, etc. Complicated magnetic structure of BFO at below room temperature may open up further study which then important to understand another multiferroic system.

Acknowledgements

The authors gratefully acknowledge the financial support of internal funding from Universitas Airlangga and the Ministry of Science and Technology of Taiwan.

References

- [1] M. Bibes and A. Barthélemy, "Towards a magnetoelectric memory," *Nat. Mater.*, vol. 7, no. 6, pp. 425–426, Jun. 2008, doi: 10.1038/nmat2189.
- [2] L. W. Martin, Y.-H. Chu, and R. Ramesh, "Advances in the growth and characterization of magnetic, ferroelectric, and multiferroic oxide thin films," *Mater. Sci. Eng. R Reports*, vol. 68, no. 4–6, pp. 89–133, May 2010, doi: 10.1016/j.mser.2010.03.001.
- [3] T. Amrillah et al., "Preferentially Oriented Nanometer-Sized CoFe₂O₄ Mesocrystals Embedded in the BiFeO₃ Matrix for Opto-Magnetic Device Applications," *ACS Appl. Nano Mater.*, p. acsannm.1c02804, Oct. 2021, doi: 10.1021/acsnm.1c02804.

- [4] D. Sando *et al.*, "Crafting the magnonic and spintronic response of BiFeO₃ films by epitaxial strain," *Nat. Mater.*, vol. 12, no. 7, pp. 641–646, Jul. 2013, doi: 10.1038/nmat3629.
- [5] K.-T. Ko *et al.*, "Concurrent transition of ferroelectric and magnetic ordering near room temperature," *Nat. Commun.*, vol. 2, no. 1, p. 567, Sep. 2011, doi: 10.1038/ncomms1576.
- [6] A. J. Hatt, N. A. Spaldin, and C. Ederer, "Strain-induced isosymmetric phase transition in BiFeO₃," *Phys. Rev. B*, vol. 81, no. 5, p. 054109, Feb. 2010, doi: 10.1103/PhysRevB.81.054109.
- [7] R. Ramesh and N. A. Spaldin, "Multiferroics: progress and prospects in thin films," *Nat. Mater.*, vol. 6, no. 1, pp. 21–29, Jan. 2007, doi: 10.1038/nmat1805.
- [8] K. Sone, H. Naganuma, T. Miyazaki, T. Nakajima, and S. Okamura, "Crystal Structures and Electrical Properties of Epitaxial BiFeO₃ Thin Films with (001), (110), and (111) Orientations," *Jpn. J. Appl. Phys.*, vol. 49, no. 9, p. 09MB03, Sep. 2010, doi: 10.1143/JJAP.49.09MB03.
- [9] D. Chiba, N. Shibata, and A. Tsukazaki, "Co thin films deposited directly on ZnO polar surfaces," *Sci. Rep.*, vol. 6, no. 1, p. 38005, Dec. 2016, doi: 10.1038/srep38005.
- [10] Y.-M. Yu and B.-G. Liu, "Contrasting morphologies of O-rich ZnO epitaxy on Zn- and O-polar thin film surfaces: Phase-field model," *Phys. Rev. B*, vol. 77, no. 19, p. 195327, May 2008, doi: 10.1103/PhysRevB.77.195327.
- [11] G. Catalan and J. F. Scott, "Physics and Applications of Bismuth Ferrite," *Adv. Mater.*, vol. 21, no. 24, pp. 2463–2485, Jun. 2009, doi: 10.1002/adma.200802849.
- [12] K. C. Verma and R. K. Kotnala, "Tailoring the multiferroic behavior in BiFeO₃ nanostructures by Pb doping," *RSC Adv.*, vol. 6, no. 62, pp. 57727–57738, 2016, doi: 10.1039/C6RA12949H.